Published in Organometallics 28, issue 15, pp. 4350–4357, 2009,
which should be used for any reference to this work

Synthesis, Molecular Structure, and Anticancer Activity of Cationic Arene Ruthenium Metallarectangles

Johan Mattsson,[†] Padavattan Govindaswamy,[†] Anna K. Renfrew,[‡] Paul J. Dyson,[‡] Petr Štěpnička,[§] Georg Süss-Fink,[†] and Bruno Therrien*,[†]

[†]*Institut de Chimie, Université de Neuchâtel, Case Postale 158, CH-2009 Neuchâtel, Switzerland, Institut des Sciences et*
[‡]*Ingénierie Chimiques, Ecole Polytechnique Fédérale de Lausanne (EPFL), CH-1015, Lausanne, Switzerland*
[§]*Department of Inorganic Chemistry, Faculty of Science, Charles University, Hlavova 2030, CZ-12840, Prague 2, Czech Republic*

Cationic arene ruthenium-based tetranuclear complexes comprising rectangular structures have been obtained from the dinuclear arene ruthenium complexes $[Ru_2(arene)_2(OO\cap OO)_2Cl_2]$ (arene = *p*-cymene, hexamethylbenzene; $OO\cap OO$=2,5-dihydroxy-1,4-benzoquinonato, 2,5-dichloro-1,4-benzo-quinonato) by reaction with pyrazine or bipyridine linkers ($N\cap N$ = pyrazine, 4,4′-bipyridine, 1,2-bis(4-pyridyl)ethylene) in methanol in the presence of AgO_3SCF_3, forming tetranuclear cations of general for-mula $[Ru_4(arene)_4(N\cap N)_2(OO\cap OO)_2]^{4+}$. All complexes were isolated in good yield as triflate salts and were characterized by NMR and IR spectroscopy and studied by cyclic voltammetry. The cytotoxicities of the water-soluble compounds of the 4,4′-bipyridine and 1,2-bis(4-pyridyl)ethylene series have been established using ovarian A2780 cancer cells. The large rectangles incorporating 1,2-bis(4-pyridyl)-ethylene linkers are ca. 5 times more cytotoxic ($IC_{50} \leq 6\ \mu M$) than the 4,4′-bipyridine-containing cations ($IC_{50} \geq 30\ \mu M$). Structural characterization by X-ray diffraction of two representative compounds, i.e., the triflate salts of $[Ru_4(hexamethylbenzene)_4(4,4'\text{-bipyridine})_2(2,5\text{-dihydroxy-}1,4\text{-benzoquinonato})_2]^{4+}$ and $[Ru_4(hexamethylbenzene)_4(1,2\text{-bis(4-pyridyl)ethylene})_2(2,5\text{-dichloro-}1,4\text{-benzoquinonato})_2]^{4+}$, re-veals differently sized cavities, different flexibilities, and different packing arrangements, suggesting a correlation between these structural properties and the observed cytotoxicities.

Introduction

The self-assembly of transition metal complexes with polydentate ligands to give discrete supramolecular assemblies has been studied by several groups. Notably, in the 1990s,[1] Fujita pioneered, and others subsequently used,[2] the combination of 90° coordination building blocks and ditopic linear ligands to form square and rectangular architectures. A few years later, a related approach was used to generate three-dimensional networks.[3] So far, a multitude of two- and three-dimensional supramolecular structures incorporating square-planar transition metal ions have been synthesized.[4] These molecular architectures are very versatile and have been used to generate confined environments that encapsulate compounds,[5] protect and stabilize an otherwise unstable molecule,[6] inhibit telomerase by stabilizing G-quadruplexes,[7] recognize and trap specific guest molecules,[8] or even act as microreactors for specific reactions.[9]

*Corresponding author. E-mail: bruno.therrien@unine.ch.

(1) Fujita, M.; Yazaki, J.; Ogura, K. *J. Am. Chem. Soc.* **1990**, *112*, 5645–5647.

(2) (a) Kuehl, C. J.; Huang, S. D.; Stang, P. J. *J. Am. Chem. Soc.* **2001**, *123*, 9634–9641. (b) Moriuchi, T.; Miyaishi, M.; Hirai, T. *Angew. Chem., Int. Ed.* **2001**, *40*, 3042–3045. (c) Das, N.; Mukherjee, P. S.; Arif, A. M.; Stang, P. J. *J. Am. Chem. Soc.* **2003**, *125*, 13950–13951. (d) Mukherjee, P. S.; Das, N.; Kryschenko, Y. K.; Arif, A. M.; Stang, P. J. *J. Am. Chem. Soc.* **2004**, *126*, 2464–2473. (e) Caskey, D. C.; Shoemaker, R. K.; Michl, J. *Org. Lett.* **2004**, *6*, 2093–2096. (f) Yoshizawa, M.; Nagao, M.; Kumazawa, K.; Fujita, M. *J. Organomet. Chem.* **2005**, *690*, 5383–5388. (g) Kim, D.; Paek, J. H.; Jun, M.-J.; Lee, J. Y.; Kang, S. O.; Ko, J. *Inorg. Chem.* **2005**, *44*, 7886–7894. (h) Northrop, B. H.; Yang, H.-B.; Stang, P. J. *Chem. Commun.* **2008**, 5896–5908.

(3) Fujita, M.; Oguro, D.; Miyazawa, M.; Oka, H.; Yamaguchi, K.; Ogura, K. *Nature* **1995**, *378*, 469–471.

(4) (a) Pirondini, L.; Bertolini, F.; Cantadori, B.; Ugozzoli, F.; Massera, C.; Dalcanale, E. *Proc. Natl. Acad. Sci. U.S.A.* **2002**, *99*, 4911–4915. (b) Ovchinnikov, M. V.; Holliday, B. J.; Mirkin, C. A.; Zakharov, L. N.; Rheingold, A. L. *Proc. Natl. Acad. Sci. U.S.A.* **2002**, *99*, 4927–4931. (c) Kuehl, C. J.; Kryschenko, Y. K.; Radhakrishnan, U.; Russell Seidel, S.; Huang, S. D.; Stang, P. J. *Proc. Natl. Acad. Sci. U.S.A.* **2002**, *99*, 4932–4936. (d) Kryschenko, Y. K.; Russell Seidel, S.; Muddiman, D. C.; Nepomuceno, A. I.; Stang, P. J. *J. Am. Chem. Soc.* **2003**, *125*, 9647–9652. (e) Crowley, J. D.; Goshe, A. J.; Bosnich, B. *Chem. Commun.* **2003**, 2824–2825. (f) Fujita, M.; Tominaga, M.; Hori, A.; Therrien, B. *Acc. Chem. Res.* **2005**, *38*, 369–378. (g) Caskey, D. C.; Michl, J. *J. Org. Chem.* **2005**, *70*, 5442–5448. (h) Maurizot, V.; Yoshizawa, M.; Kawano, M.; Fujita, M. *Dalton Trans.* **2006**, 2750–2756.

(5) (a) Kusukawa, T.; Fujita, M. *Angew. Chem., Int. Ed.* **1998**, *37*, 3142–3144. (b) Kusukawa, T.; Yoshizawa, M.; Fujita, M. *Angew. Chem., Int. Ed.* **2001**, *40*, 1879–1884. (c) Kusukawa, T.; Fujita, M. *J. Am. Chem. Soc.* **2002**, *124*, 13576–13582.

(6) (a) Nakabayashi, K.; Kawano, M.; Yoshizawa, M.; Ohkoshi, S.; Fujita, M. *J. Am. Chem. Soc.* **2004**, *126*, 16694–16695. (b) Kawano, M.; Kobayashi, Y.; Ozeki, T.; Fujita, M. *J. Am. Chem. Soc.* **2006**, *128*, 6558–6559. (c) Nakabayashi, K.; Kawano, M.; Kato, T.; Furukawa, T.; Ohkoshi, S.; Hozumi, T.; Fujita, M. *Chem.: Asian J.* **2007**, *2*, 164–170. (d) Ono, K.; Yoshizawa, M.; Akita, M.; Kato, T.; Tsunobuchi, Y.; Ohkoshi, S.; Fujita, M. *J. Am. Chem. Soc.* **2009**, *131*, 2782–2783. (e) Sawada, T.; Yoshizawa, M.; Sato, S.; Fujita, M. *Nat. Chem.* **2009**, *1*, 53–56.

(7) Kieltyka, R.; Englebienne, P.; Kakhoury, J.; Autexier, C.; Moitessier, N.; Sleiman, H. F. *J. Am. Chem. Soc.* **2008**, *130*, 10040–10041.

(8) (a) Kusukawa, T.; Fujita, M. *J. Am. Chem. Soc.* **1999**, *121*, 1397–1398. (b) Yoshizawa, M.; Tamura, M.; Fujita, M. *J. Am. Chem. Soc.* **2004**, *126*, 6846–6847. (c) Tashiro, S.; Tominaga, M.; Kawano, M.; Therrien, B.; Ozeki, T.; Fujita, M. *J. Am. Chem. Soc.* **2005**, *127*, 4546–4547.

In the search for new building blocks for the synthesis of supramolecular boxes with comparable but modified properties, there has been an increasing interest in using transition metal complexes with octahedral geometry.[10] Cotton and co-workers built up two- and three-dimensional structures from metal−metal paddlewheel units.[11] Similarly, the *fac*-Re(CO)$_3$ fragment was judiciously chosen to prepare molecular rectangles[12] or triangular prisms.[13] The tridentate ligand 1,4,7-trithiacyclononane, which coordinates facially to ruthenium, has been used to form a supramolecular cube,[14] and polypyrazolyl chelating ligands coordinated to cobalt, manganese, and zinc ions can form various polyhedral cages.[15] In a similar manner, cyclopentadienyl or arene ligands can be used to control the accessibility of coordination sites of an octahedral metal center. Thus, CpM and Cp*M (M = Rh, Ir; Cp = C_5H_5; Cp* = C_5Me_5) units have been extensively used to generate metallacycles, rectangles, trigonal prisms, hexagonal prisms, and other supramolecular assemblies.[16] In addition, arene ruthenium complexes (arene = benzene, toluene, *p*-cymene, hexamethylbenzene) have been shown to afford supramolecular assemblies with diverse functionalities and properties.[17] Our first entry in the field of supramolecular assemblies of metallarectangles incorporating arene ruthenium complexes dates back to 1997. The tetranuclear complex [Ru$_4$(*p*-cymene)$_4$(4,4′-bipyridine)$_2$(oxalato)$_2$]$^{4+}$, a molecular rectangle in which four arene ruthenium units (arene = *p*-cymene) are bridged by two oxalato ligands and two bipyridine units, was synthesized from the dinuclear complex [Ru$_2$(*p*-cymene)$_2$(oxalato)Cl$_2$] and the bidentate ligand 4,4′-bipyridine (*N*∩*N*) in the presence of $AgCF_3SO_3$.[18]

Ruthenium compounds are considered as promising anticancer agents, and many compounds have been evaluated *in vitro* and *in vivo*.[19] Ru(III) compounds have recently entered clinical trials,[20] and arene ruthenium(II) complexes are at a preclinical development stage.[21] Compared to classical platinum drugs, different affinities to biomolecules appear to be of importance in the mode of action of ruthenium compounds that potentially endows them with some advantageous properties.[22]

Recently, a series of trinuclear *p*-cymene ruthenium metallacycles connected with aminomethyl-substituted 3-hydroxy-2-pyridone ligands were evaluated *in vitro* against cancer and fibroblast cell lines.[23] It was postulated that the water-soluble trinuclear complexes undergo fragmentation after uptake, thus giving rise to cytotoxic mononuclear complexes. We also reported the synthesis of water-soluble metallaprisms that are able to encapsulate planar aromatic molecules (e.g., pyrene, coronene),[24] or square-planar

(9) (a) Yoshizawa, M.; Takeyama, Y.; Kusukawa, T.; Fujita, M. *Angew. Chem., Int. Ed.* **2002**, *41*, 1347–1349. (b) Yoshizawa, M.; Tamura, M.; Fujita, M. *Science* **2006**, *312*, 251–254. (c) Yamaguchi, T.; Fujita, M. *Angew. Chem., Int. Ed.* **2008**, *47*, 2067–2069. (d) Nishioka, Y.; Yamaguchi, T.; Kawano, M.; Fujita, M. *J. Am. Chem. Soc.* **2008**, *130*, 8160–8161.

(10) (a) Caulder, D. L.; Raymond, K. N. *Acc. Chem. Res.* **1999**, *32*, 975–982. (b) Mukherjee, P. S.; Min, K. S.; Arif, A. M.; Stang, P. J. *Inorg. Chem.* **2004**, *43*, 6345–6350. (c) Mahmoudkhani, A. H.; Cté, A. P.; Shimizu, G. K. H. *Chem. Commun.* **2004**, 2678–2679. (d) Fiedler, D.; Leung, D. H.; Bergman, R. G.; Raymond, K. N. *Acc. Chem. Res.* **2005**, *38*, 351–360. (e) Pluth, M. D.; Raymond, K. N. *Chem. Soc. Rev.* **2007**, *36*, 161–171. (f) Pluth, M. D.; Johnson, D. W.; Szigethy, G.; Davis, A. V.; Teat, S. J.; Oliver, A. G.; Bergman, R. G.; Raymond, K. N. *Inorg. Chem.* **2009**, *48*, 111–120.

(11) (a) Cotton, F. A.; Lin, C.; Murillo, C. A. *Acc. Chem. Res.* **2001**, *34*, 759–771. (b) Cotton, F. A.; Murillo, C. A. *Eur. J. Inorg. Chem.* **2006**, 4209–4218. (c) Donahue, J. P.; Murillo, C. A. *Dalton Trans.* **2008**, 1547–1551. (d) Cotton, F. A.; Jin, J.-Y.; Li, Z.; Murillo, C. A.; Reibenspies, J. H. *Chem. Commun.* **2008**, 211–213.

(12) (a) Woessner, S. M.; Helms, J. B.; Shen, Y.; Sullivan, B. P. *Inorg. Chem.* **1998**, *37*, 5406–5407. (b) Rajendran, T.; Manimaran, B.; Lee, F.-Y.; Lee, G.-H.; Peng, S.-M.; Wang, C. M.; Lu, K.-L. *Inorg. Chem.* **2000**, *39*, 2016–2017. (c) Sun, S.-S.; Silva, A. S.; Brinn, I. M.; Lees, A. J. *Inorg. Chem.* **2000**, *39*, 1344–1345. (d) Rajendran, T.; Manimaran, B.; Lee, F.-Y.; Chen, P.-J.; Lin, S.-C.; Lee, G.-H.; Peng, S.-M.; Chen, Y.-J.; Lu, K.-L. *J. Chem. Soc., Dalton Trans.* **2001**, 3346–3351. (e) Sun, S.-S.; Lees, A. J. *Inorg. Chem.* **2001**, *40*, 3154–3160. (f) Rajendran, T.; Manimaran, B.; Liao, R.-T.; Lin, R.-J.; Thanasekaran, P.; Lee, G.-H.; Peng, S.-M.; Liu, Y.-H.; Chang, I.-J.; Rajagopal, S.; Lu, K.-L. *Inorg. Chem.* **2003**, *42*, 6388–6394.

(13) (a) Benkstein, K. D.; Hupp, J. T.; Stern, C. L. *J. Am. Chem. Soc.* **1998**, *120*, 12982–12983. (b) Benkstein, K. D.; Hupp, J. T. *Mol. Cryst. Liq. Cryst.* **2000**, *342*, 151–158. (c) Manimaran, B.; Rajendran, T.; Lu, Y.-L.; Lee, G.-H.; Peng, S.-M.; Lu, K.-L. *Eur. J. Inorg. Chem.* **2001**, 633–636. (d) Sun, S.-S.; Lees, A. J. *Chem. Commun.* **2001**, 103–104. (e) Manimaran, B.; Thanasekaran, P.; Rajendran, T.; Liao, R.-T.; Liu, Y.-H.; Lee, G.-H.; Peng, S.-M.; Rajagopal, S.; Lu, K.-L. *Inorg. Chem.* **2003**, *42*, 4795–4797.

(14) (a) Roche, S.; Haslam, C.; Adams, H.; Heath, S. L.; Thomas, J. A. *Chem. Commun.* **1998**, 1681–1682. (b) Roche, S.; Spey, S. E.; Adams, H.; Thomas, J. A. *Inorg. Chim. Acta* **2001**, *323*, 157–162.

(15) (a) Ward, M. D. In *Organic Nanostructures*; Atwood, J. L., Steed, J. W., Eds.; Wiley-VCH: Weinheim, 2008; pp 223−250. (b) Tidmarsh, I. S.; Taylor, B. F.; Hardie, M. J.; Russo, L.; Clegg, W.; Ward, M. D. *New J. Chem.* **2008**, *33*, 366–375.

(16) (a) Smith, D. P.; Baralt, E.; Morales, B.; Olmstead, M. M.; Maestre, M. F.; Fish, R. H. *J. Am. Chem. Soc.* **1992**, *114*, 10647–10649. (b) Ogo, S.; Nakamura, S.; Chen, H.; Isobe, K.; Watanabe, Y.; Fish, R. H. *J. Org. Chem.* **1998**, *63*, 7151–7156. (c) Annen, P.; Schildberg, S.; Sheldrick, W. S. *Inorg. Chim. Acta* **2000**, *307*, 115–124. (d) Yamanari, K.; Yamamoto, S.; Ito, R.; Kushi, Y.; Fuyuhiro, A.; Kubota, N.; Fukuo, T.; Arakawa, R. *Angew. Chem., Int. Ed.* **2001**, *40*, 2268–2271. (e) Yamanari, K.; Ito, R.; Yamamoto, S.; Fuyuhiro, A. *Chem. Commun.* **2001**, 1414–1415. (f) Amouri, H.; Rager, M. N.; Cagnol, F.; Vaissermann, J. *Angew. Chem., Int. Ed.* **2001**, *40*, 3636–3638. (g) Fish, R. H.; Jaouen, G. *Organometallics* **2003**, *22*, 2166–2177. (h) Mimassi, L.; Guyard-Duhayon, C.; Rager, M. N.; Amouri, H. *Inorg. Chem.* **2004**, *43*, 6644–6649. (i) Han, Y.-F.; Lin, Y.-J.; Jia, W.-G.; Weng, L.-H.; Jin, G.-X. *Organometallics* **2007**, *26*, 5848–5853. (j) Han, Y.-F.; Jia, W.-G.; Lin, Y.-J.; Jin, G.-X. *J. Organomet. Chem.* **2008**, *693*, 546–550. (k) Mirtschin, S.; Krasniqi, E.; Scopelliti, R.; Severin, K. *Inorg. Chem.* **2008**, *47*, 6375–6381. (l) Han, Y.-F.; Jia, W.-G.; Lin, Y.-J.; Jin, G.-X. *Angew. Chem., Int. Ed.* **2009**, DOI: 10.1002/anie.200805949.

(17) (a) Korn, S.; Sheldrick, W. S. *J. Chem. Soc., Dalton Trans.* **1997**, 2191–2200. (b) Korn, S.; Sheldrick, W. S. *Inorg. Chim. Acta* **1997**, *254*, 85–91. (c) Yamanari, K.; Ito, R.; Yamamoto, S.; Konno, T.; Fuyuhiro, A.; Fujioka, K.; Arakawa, R. *Inorg. Chem.* **2002**, *41*, 6824–6830. (d) Grote, Z.; Scopelliti, R.; Severin, K. *J. Am. Chem. Soc.* **2004**, *126*, 16959–16972. (e) Severin, K. *Chem. Commun.* **2006**, 3859–3867. (f) Grote, Z.; Bonazzi, S.; Scopelliti, R.; Severin, K. *J. Am. Chem. Soc.* **2006**, *128*, 10382–10383. (g) Olivier, C.; Grote, Z.; Solari, E.; Scopelliti, R.; Severin, K. *Chem. Commun.* **2007**, 4000–4002. (h) Boyer, L.; Kuhlman, M. L.; Rauchfuss, T. B. *Acc. Chem. Res.* **2007**, *40*, 233–242. (i) Rauchfuss, T. B.; Severin K. In *Organic Nanostructures*; Atwood, J. L., Steed, J. W., Eds.; Wiley-VCH: Weinheim, 2008; pp 179−203. (j) Olivier, C.; Scopelliti, R.; Severin, K. *Eur. J. Inorg. Chem.* **2009**, 207–210.

(18) Yan, H.; Süss-Fink, G.; Neels, A.; Stoeckli-Evans, H. *J. Chem. Soc., Dalton Trans.* **1997**, 4345–4350.

(19) For reviews see: (a) Yan, Y. K.; Melchart, M.; Habtemariam, A.; Sadler, P. J. *Chem. Commun.* **2005**, 4764–4776. (b) Hartinger, C. G.; Zorbas-Seifried, S.; Jakupec, M. A.; Kynast, B.; Zorbas, H.; Keppler, B. K. *J. Inorg. Biochem.* **2006**, *100*, 891–904. (c) Ronconi, L.; Sadler, P. J. *Coord. Chem. Rev.* **2007**, *251*, 1633–1648. (d) Hartinger, C. G.; Dyson, P. J. *Chem. Soc. Rev.* **2009**, *38*, 391–401.

(20) (a) Sava, G.; Capozzi, I.; Bergamo, A.; Gagliardi, R.; Cocchietto, M.; Masiero, L.; Onisto, M.; Alessio, E.; Mestroni, G.; Garbisa, S. *Int. J. Cancer* **1996**, *68*, 60–66. (b) Galanski, M.; Arion, V. B.; Jakupec, M. A.; Keppler, B. K. *Curr. Pharm. Des.* **2003**, *9*, 2078–2089. (c) Rademaker-Lakhai, J. M.; van den Bongard, D.; Pluim, D.; Beijnen, J. H.; Schellens, J. H. M. *Clin. Cancer Res.* **2004**, *10*, 3717–3727. (d) Reisner, E.; Arion, V. B.; Guedes da Silva, M. F. C.; Lichtenecker, R.; Eichinger, A.; Keppler, B. K.; Kukushkin, V. Y.; Pombeiro, A. J. L. *Inorg. Chem.* **2004**, *43*, 7083–7093. (e) Ang, W. H.; Dyson, P. J. *Eur. J. Inorg. Chem.* **2006**, 4003–4018.

(21) Dyson, P. J. *Chimia* **2007**, *61*, 698–703.

(22) (a) Gaiddon, C.; Jeannequin, P.; Bischoff, P.; Pfeffer, M.; Sirlin, C.; Loeffler, J. P. *J. Pharmacol. Exp. Ther.* **2005**, *315*, 1403–1411. (b) Chatterjee, S.; Kundu, S.; Bhattacharyya, A.; Hartinger, C. G.; Dyson, P. J. *J. Biol. Inorg. Chem.* **2008**, *13*, 1149–1155. (c) Bergamo, A.; Masi, A.; Dyson, P. J.; Sava, G. *Int. J. Oncol.* **2008**, *33*, 1281–1289.

(23) Ang, W. H.; Grote, Z.; Scopelliti, R.; Juillerat-Jeanneret, L.; Severin, K.; Dyson, P. J. *J. Organomet. Chem.* **2009**, *694*, 968–972.

(24) Mattsson, J.; Govindaswamy, P.; Furrer, J.; Sei, Y.; Yamaguchi, K.; Süss-Fink, G.; Therrien, B. *Organometallics* **2008**, *27*, 4346–4356.

Scheme 1. Dinuclear Arene Ruthenium Complexes 1−4

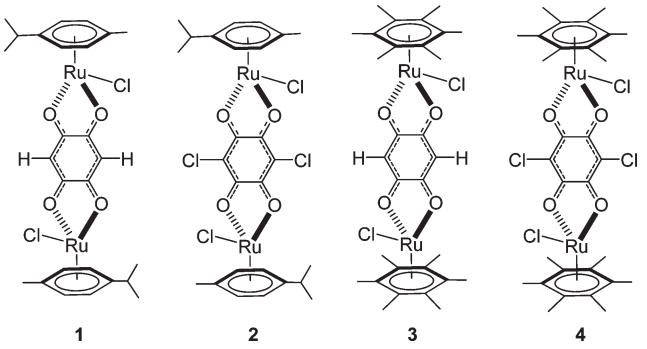

complexes (e.g., $[Pd(acac)_2]$, $[Pt(acac)_2]$),[25] synthesized from the dinuclear arene ruthenium complexes $[Ru_2(arene)_2(OO\cap OO)_2Cl_2]$ (arene = *p*-cymene, hexamethylbenzene; $OO\cap OO$ = 2,5-dihydroxy-1,4-benzoquinonato, 2,5-dichloro-1,4-benzoquinonato) and 2,4,6-tri(4-pyridyl)-1,3,5-triazine (4-tpt). The "complex-in-a-complex" systems, $[M(acac)_2\subset Ru_6(p\text{-cymene})_6(4\text{-tpt})_2(2,5\text{-dihydroxy-1,4-benzoquinonato})_3]^{6+}$ (M = Pd, Pt), showed high cytotoxicity toward human ovarian cancer cells.[25]

In this paper we describe the synthesis of some tetranuclear metallarectangles of the general formula $[Ru_4(arene)_4(N\cap N)_2(OO\cap OO)_2]^{4+}$ (arene = *p*-cymene, hexamethylbenzene; $OO\cap OO$ = 2,5-dihydroxy-1,4-benzoquinonato, 2,5-dichloro-1,4-benzoquinonato; $N\cap N$ = pyrazine, 4,4′-bipyridine, 1,2-bis(4-pyridyl)ethylene), prepared from the dinuclear arene ruthenium complexes **1**−**4**;[24,25] see Scheme 1. The synthesis, characterization (including X-ray structure analysis), and *in vitro* anticancer activity of these arene ruthenium-based metallarectangles is reported together with their electrochemical behavior.

Results and Discussion

The dinuclear arene ruthenium complexes $[Ru_2(arene)_2(OO\cap OO)Cl_2]$ (**1**−**4**) react in methanol at room temperature in the presence of silver triflate as a halide scavenger with different $N\cap N$ donor ligands ($N\cap N$ = pyrazine, 4,4′-bipyridine, 1,2-bis(4-pyridyl)ethylene) to give the metallacyclic tetranuclear cations **5**−**16** stabilized as the triflate salts (see Scheme 2). The chlorinated derivatives **6**, **10**, and **14** have also been synthesized by G.-X. Jin and co-workers and reported recently.[26] Compounds **1**−**4** and **[9**−**16]**$[CF_3SO_3]_4$ are soluble in polar organic solvents such as dichloromethane, acetone, methanol, or dimethylsulfoxide and also in water. On the other hand, compounds **[5**−**8]**$[CF_3SO_3]_4$ dissolve only sparingly in acetone and dichloromethane and show rapid decomposition in dimethylsulfoxide.

The ^{1}H NMR spectra of **5**−**8** display a singlet due to the pyrazine protons. Unlike free pyrazine, where the proton signal is found at δ_H = 8.61 in acetone-d_6, the signal in **5**−**8** appears slightly shifted downfield to δ_H = 8.7 ppm. Upon formation of the cationic tetranuclear metallarectangles, the methyl and isopropyl signals of the *p*-cymene ligands in **5**, **6**, **9**, **10**, **13**, and **14** remain almost unchanged as compared to complexes **1** and **2**, while the aromatic protons of the

Scheme 2. Synthesis of the Metallarectangles 5−16

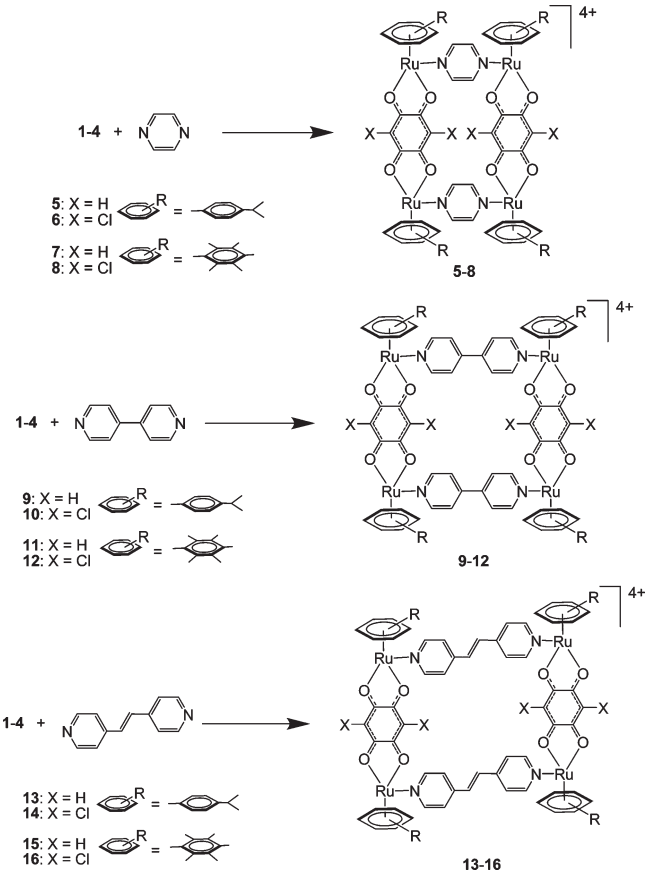

p-cymene ligands are shifted downfield. On the other hand, the proton signal of the 2,5-dihydroxy-1,4-benzoquinonato bridging ligands in **5**, **7**, **9**, **11**, **13**, and **15** is shifted upfield as compared to the parent complexes **1** and **3**. The infrared spectra of **5**−**16** are dominated by absorptions of the coordinated $N\cap N$ and $OO\cap OO$ ligands, which are only slightly shifted as compared to the free ligands. In addition to the $N\cap N$ and $OO\cap OO$ signals, strong absorptions due to the triflate anions [1260(s), 1030(s), 638(m) cm^{-1}] are also observed in the infrared spectra of the salts **[5**−**16]**$[CF_3SO_3]_4$.

The single-crystal X-ray structure analysis of **[11]**$[CF_3SO_3]_4$ and **[16]**$[CF_3SO_3]_4$ confirms the expected rectangular structures. The molecular structures are presented in Figures 1 and 2, respectively, along with selected geometrical parameters.

Cations **11** and **16** contain four ruthenium metal centers bonded to a hexamethylbenzene ligand, which are bridged by the dianionic $OO\cap OO$ ligand through its four oxygen atoms and linked by the neutral $N\cap N$ ligand. The Ru−N and Ru−O distances observed in **11** and **16** are comparable to those found in the hexacationic metallaprisms $[guest\subset Ru_6(arene)_6(4\text{-tpt})_2(2,5\text{-dihydroxy-1,4-benzoquinonato})_3][CF_3SO_3]_6$ (guest = pyrene, benzo[*e*]pyrene, Pt(acetylacetonato)$_2$, hexamethoxytriphenylene).[24,25,27] In **11** the 4,4′-bipyridine linkers show a twist of 4.6° between the two pyridyl units, which is comparable to that found in other 4,4′-bipyridine-bridged ruthenium complexes.[28]

(25) Therrien, B.; Süss-Fink, G.; Govindaswamy, P.; Renfrew, A. K.; Dyson, P. J. *Angew. Chem., Int. Ed.* **2008**, *47*, 3773–3776.
(26) Han, Y.-F.; Jia, W.-G.; Lin, Y.-J.; Jin, G.-X. *Organometallics* **2008**, *27*, 5002–5008.
(27) Govindaswamy, P.; Furrer, J.; Süss-Fink, G.; Therrien, B. *Z. Anorg. Allg. Chem.* **2008**, *634*, 1349–1352.
(28) Berben, L. A.; Faia, M. C.; Crawford, N. R. M.; Long, J. R. *Inorg. Chem.* **2006**, *45*, 6378–6386.

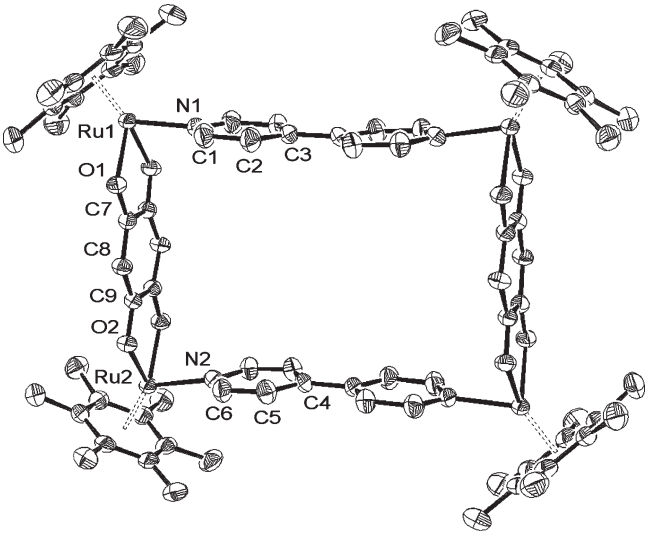

Figure 1. ORTEP representation of cation **11** at 35% probability level with H atoms omitted for clarity. Selected bond lengths (Å) and angles (deg): Ru(1)−O(1) 2.086(3), Ru(2)−O(2) 2.089(3), Ru(1)−N(1) 2.109(4), Ru(2)−N(2) 2.109(4); N(1)−Ru(1)−O(1) 84.13(12), O(1)−Ru(1)−O(1)^{i} 77.24(14), N(2)−Ru(2)−O(2) 84.56(12), O(2)−Ru(2)−O(2)^{i} 77.18(14) ($i = x, -y, z$).

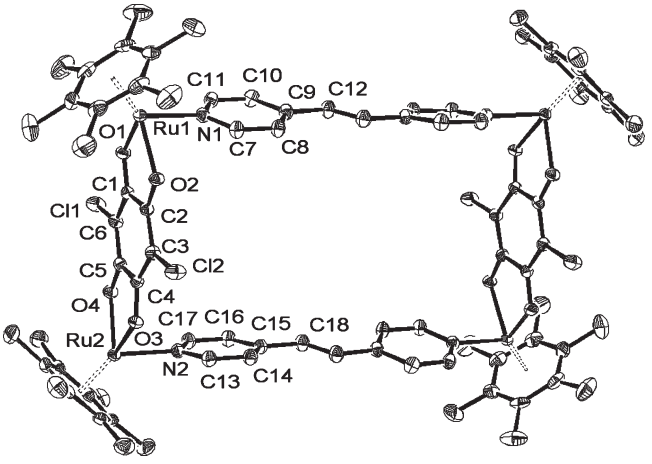

Figure 2. ORTEP representation of cation **16** at 35% probability level with H atoms omitted for clarity. Selected bond lengths (Å) and angles (deg): Ru(1)−N(1) 2.108(2), Ru(1)−O(1) 2.0927(18), Ru(1)−O(2) 2.0837(18), Ru(2)−N(2) 2.111(2), Ru(2)−O(3) 2.0965(18), Ru(2)−O(4) 2.0937(18); N(1)−Ru(1)−O(1) 86.53(8), N(1)−Ru(1)−O(2) 84.08(8), O(1)−Ru(1)−O(2) 77.12(7), N(2)−Ru(2)−O(3) 82.75(8), N(2)−Ru(2)−O(4) 86.27(8), O(3)−Ru(2)−O(4) 76.93(7).

Interestingly, [**11**][CF_3SO_3]$_4$ forms in the solid state one-dimensional channels along the *b* axis with intramolecular Ru−Ru separations of 7.9 and 11.3 Å (Figure 3). A similar arrangement along the *c* axis has been found in the crystal structure of [**10**][CF_3SO_3]$_4$, with almost identical Ru−Ru separations (7.9 and 11.2 Å).[26] In both structures the triflate anions are located between the rectangular channels. However, in [**10**][CF_3SO_3]$_4$ disordered water molecules are observed in the cationic molecular rectangle as compared to [**11**][CF_3SO_3]$_4$ for which no solvent molecules are observed in the hydrophobic cavity. As expected, the molecular structure of [**16**][CF_3SO_3]$_4$ shows a larger cavity (7.9 × 13.6 Å^2). Upon crystallization of [**16**][CF_3SO_3]$_4$ from a chloroform/diethyl ether mixture, two diethyl ether molecules are encompassed in the hydrophobic cavity of cation **16** (Figure 3). A similar crystal packing has been observed in [**14**][CF_3SO_3]$_4$ in which highly disordered solvent molecules were found in the rectangular 7.9 × 13.5 Å^2 cavity.[26]

Compounds **1**−**4** and [**9**−**16**][CF_3SO_3]$_4$ have been studied by cyclic voltammetry at a platinum disk electrode. The measurements were performed on ca. 0.5 mM (or saturated) dichloromethane solutions containing 0.1 M Bu_4NPF_6 as the supporting electrolyte. Pertinent data are summarized in Table 1.

The redox response of the dinuclear complexes **1**−**4** is roughly similar, the compounds displaying one or two well-separated oxidations and one or two reductions in the accessible potential range. Unfortunately, the reduction waves are difficult to study, as they occur at the upper limit of the potential window provided by the solvent.

Complex **1** shows two well-separated irreversible reductions at −1.20 and −1.89 V and an oxidation at around +1.0 V (Figure 4). Replacement of 2,5-dihydroxy-1,4-benzoquinonato with 2,5-dichloro-1,4-benzoquinonato bridges such as in **2** results in a shift of the reductive waves to less negative potentials while making the single oxidation more difficult (Table 1). In addition, the presence of the 2,5-dichloro-1,4-benzoquinonato ligand renders the first reduction wave reversible (Figure 4). The wave is observed with full electrochemical reversibility when recorded with the switching potential set before the second reduction process at scan rates down to 0.1 V s^{-1}. However, upon extending the scan range further beyond the second reduction wave, the anodic peak current due to the first wave becomes lower than its corresponding cathodic counterpeak. This points to some coupled chemical processes that consume the electrogenerated species and is in accordance with the fact that the second reduction is accompanied by adsorption processes or decomposition.

The replacement of the *p*-cymene ligand for hexamethylbenzene (**1** → **3** and **2** → **4**) leaves the redox pattern virtually unchanged, but the respective waves appear shifted to more negative potentials. Apparently, the higher donor ability of the hexamethylbenzene ligand makes any electron addition more difficult while facilitating the oxidative processes. For **3**, this "shift" allows for observation of two oxidative waves at +0.76 and ca. +1.1 V, whereas the expected second reduction falls outside the accessible potential range.

In analogy to the previous reports dealing with electrochemistry of diruthenium complexes featuring 2,5-dihydroxy-1,4-benzoquinonato and 2,5-dichloro-1,4-benzoquinonato bridges,[29,30] we can formally assign the cathodic processes to one-electron reductions that occur predominantly at the bridging ligand and attribute the oxidations to the Ru(II)/Ru(III) couples. Nevertheless, this assignment is only qualitative, particularly if one considers the extensive mixing of the metal-based orbitals with those located at the bridging ligands as established by theoretical calculations.[30a]

(29) Kitagawa, S.; Kawata, S. *Coord. Chem. Rev.* **2002**, *224*, 11–34.
(30) (a) Ward, M. D. *Inorg. Chem.* **1996**, *35*, 1712–1714. (b) Gupta, A. K.; Gupta, A.; Choudhury, A. *Indian J. Chem.* **2002**, *41A*, 2076–2078. For osmium analogues, see: (c) Gupta, P.; Das, A.; Basuli, F.; Castineiras, A.; Sheldrick, W. S.; Mayer-Figge, H.; Bhattacharya, S. *Inorg. Chem.* **2005**, *44*, 2081–2088. For iridium analogues, see: (d) Lin, Y.-J.; Jia, W.-G.; Jin, G.-X. *Organometallics* **2008**, *27*, 4088–4097.

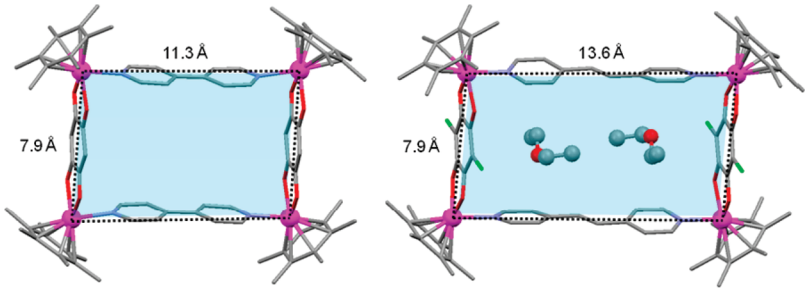

Figure 3. Capped sticks representations of **11** (left) and [(diethyl ether)$_2$⊂**16**] (right).

Table 1. Summary of the Electrochemical Data of Complexes 1−4 and 9−16[a]

compound	E [V]
1	−1.20 (ir.), −1.89 (ir.); ca. +1.0 (ir.)
2	−0.90 (rev.), −1.76 (ir.),[b] ca. +1.1 (ir.)
3	−1.37 (ir.), +0.76 (ir.), ca. +1.1 (ir.)
4	−1.06 (rev.), ca. −2.0 (ir.), ca. +0.76 (ir.)
[**9**][CF_3SO_3]$_4$	−0.68 (rev.),[c] −1.39 (ir.), −1.90 (ir.)
[**10**][CF_3SO_3]$_4$	−0.45 (rev.),[c] −1.15 (rev.)[c,d]
[**11**][CF_3SO_3]$_4$	−0.82 (rev.)[c], ca. −1.6 (ir.)
[**12**][CF_3SO_3]$_4$	−0.55 (rev.), −1.35 (rev.)[c]
[**13**][CF_3SO_3]$_4$	−0.70 (rev.), −1.42 (ir.), ca. −1.9 (ir.)
[**14**][CF_3SO_3]$_4$	−0.45 (rev.), −1.19 (rev.)[c], ca. −1.9 (ir.)
[**15**][CF_3SO_3]$_4$	−0.56 (rev.),[c] −1.44 (ir.)
[**16**][CF_3SO_3]$_4$	−0.57 (rev.),[c] −1.41 (rev.)[c], ca. −2.0 (ir.)

[a] Potentials are given relative to ferrocene/ferrocenium. Peak potentials are quoted for irreversible (ir.) processes (E_{pa} or E_{pc}). The potentials for reversible (rev.) couples are defined as the mean of the anodic and cathodic peak potentials: $E^{\circ\prime} = 1/2(E_{pa} + E_{pc})$. [b] A prepeak is observed at −1.65 V. [c] See text. [d] The most negative peak is hidden by decomposition of the base electrolyte and some decomposition processes.

Like in the case of the dinuclear compounds, the overall redox response of the tetraruthenium complexes **9**−**16** is analogous. Compared with their diruthenium precursors, complexes **9**−**16** bear a high positive charge and, hence, are more prone to reduction, whereas their oxidative waves are either observed at the onset of the base electrolyte decomposition (**13**) or not observed at all due to their highly positive redox potentials.

The *p*-cymene ruthenium complex possessing 4,4′-bipyridine bridges, compound **9**, undergoes first a reversible reduction at −0.68 V followed by two successive irreversible reductions at −1.39 and −1.90 V (Figure 5). The following redox steps apparently influence the first one: When the scanning is performed just over the first reduction, the first reduction is observed with full electrochemical reversibility. Upon increasing the switching potential so that the scan involves the subsequent redox step(s), the oxidative peak due to the first wave is observed with a significantly lower peak current. This again points to some associated follow-up associated processes that consume the electrogenerated product(s).

The behavior of the analogous compound **13** featuring 1,2-bis(4-pyridyl)ethylene linkers is practically identical, except that all the waves are shifted to slightly more negative potentials. By contrast, the change of the bridge for the 2,5-dichloro-1,4-benzoquinonato anion has a more pronounced effect. The first two waves in **10** and **14** (Figure 5) are observed shifted to more positive potentials, which is in accordance with the electron-withdrawing nature of the chloride substituents replacing two hydrogen atoms at the *OO*∩*OO* bridging ligand. In addition, both waves bear clear signs of electrochemical reversibility, the first wave being observed with full reversibility when the switching potential is set just after the first reduction. The following wave can be described as quasi-reversible, showing a lower peak current for the back scan peak (anodic) than for the forward (cathodic) peak ($i_{pc} > i_{pa}$). Moreover, scanning further beyond the second wave (i.e., toward more negative potentials) markedly lowers the reversibility of the first redox step, causing an increase in the separation of the counterpeaks and lowering of the current of the respective anodic counterwave.

The redox behavior of **11**−**15** and **12**−**16** is complicated by adsorption phenomena that become particularly pronounced upon repeated scanning and reduce the reversibility and reproducibility of the cyclic voltammograms. This is particularly the case of **15**, which shows additional ill-defined reductive peaks and a strong stripping peak in the anodic region.

The antiproliferative activity of the water-soluble compounds containing the ligands 4,4′-bipyridine (**9**−**12**) and 1,2-bis(4-pyridyl)ethylene (**13**−**16**) was evaluated against the A2780 ovarian cancer cell line. All complexes exhibit moderate to excellent activity with IC_{50} values in the range 4−66 μM (Table 2). In each case, the hexamethylbenzene complexes exhibit lower IC_{50} values than their *p*-cymene analogues, probably resulting from increased uptake due to their greater lipophilicity. Similarly, complexes containing the dihydroquinone linkers are generally more active than the less lipophilic dichloroquinone analogues. There does not appear to be a correlation between the redox potentials of the compounds and their cytotoxicity, which is perhaps not surprising since it is generally considered that Ru(III) compounds are reduced to Ru(II) compounds[31] inside the reductive environment of a tumor (with Ru(0) not biologically accessible), and therefore the compounds investigated herein are already in the active oxidation state.

Interestingly, the large rectangles incorporating 1,2-bis(4-pyridyl)ethylene and 2,5-dihydroxy-1,4-benzoquinonato linkers (complexes **13** and **15**) are up to an order of magnitude more cytotoxic ($IC_{50} \leq 6\ \mu$M) than the 4,4′-bipyridine-containing cations ($IC_{50} \geq 30\ \mu$M). The reason for this effect is not clear but it could be linked to the increased flexibility of the 1,2-bis(4-pyridyl)ethylene linker that may allow the rectangular structures to adapt their shape to better fit with a molecular target. However, it cannot be ruled out that the tetranuclear cations fragment once inside a cell and that the fragments induce the cytotoxic effect.

In conclusion, a series of rectangular tetraruthenium tetracationic complexes have been prepared and characterized

(31) Clarke, M. J.; Zhu, F.; Frasca, D. R. *Chem. Rev.* **1999**, *99*, 2511–2533.

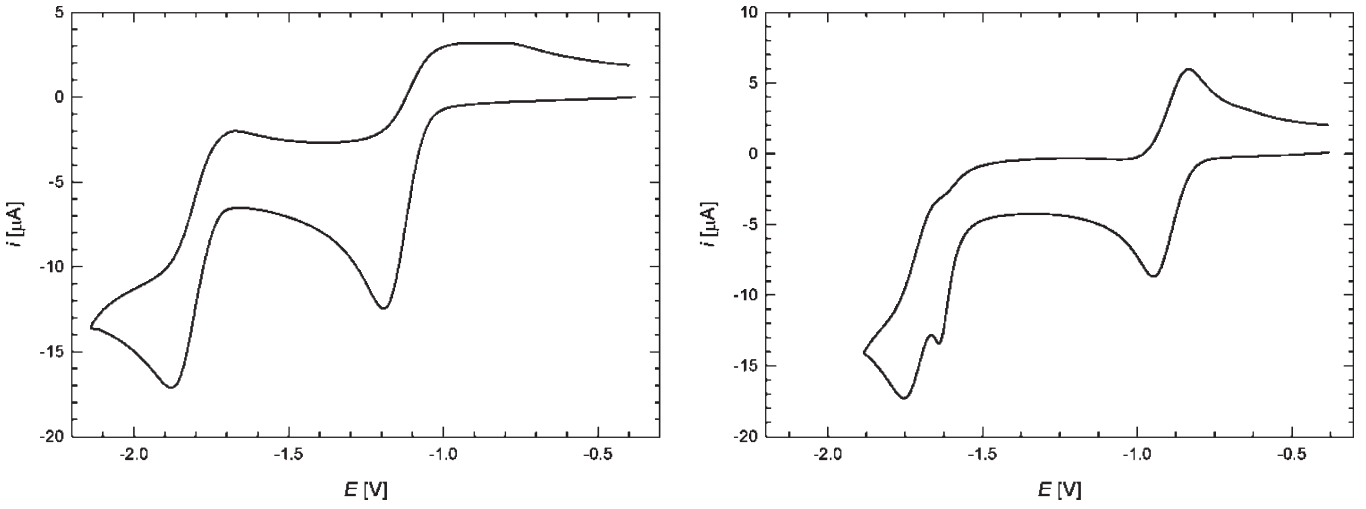

Figure 4. Cyclic voltammograms of **1** (left) and **2** (right) (0.5 mM in CH_2Cl_2 at Pt-disk, scan rate 0.1 V s^{-1}).

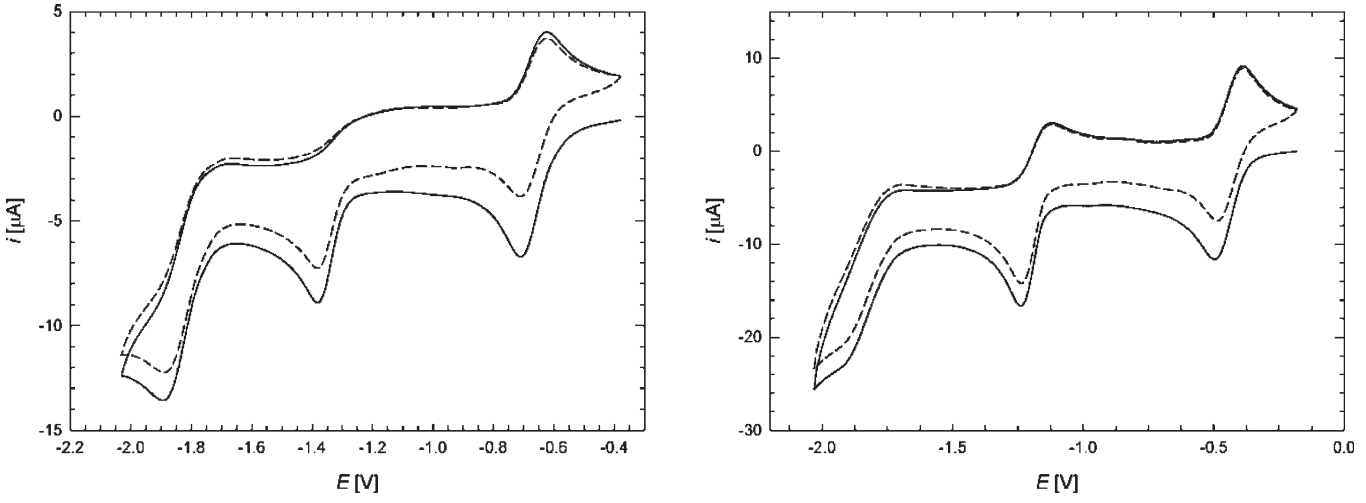

Figure 5. Cyclic voltammograms of **9** (left) and **14** (right) (0.5 mM in CH_2Cl_2 at Pt-disk, scan rate 0.1 V s^{-1}; first scan —, second scan ---).

Table 2. IC_{50} Values of Complexes 9−16 on A2780 Human Ovarian Cancer Cells after 72 h Exposure

compound	IC_{50} (μM)
[**9**][CF_3SO_3]$_4$	66
[**10**][CF_3SO_3]$_4$	43
[**11**][CF_3SO_3]$_4$	27
[**12**][CF_3SO_3]$_4$	33
[**13**][CF_3SO_3]$_4$	6
[**14**][CF_3SO_3]$_4$	29
[**15**][CF_3SO_3]$_4$	4
[**16**][CF_3SO_3]$_4$	23
cisplatin	2

by spectroscopic methods, X-ray diffraction, and cyclic voltammetry. In addition, the water-soluble species were screened for *in vitro* anticancer activity against the A2780 ovarian cancer cell line, and some of the compounds were found to be highly active. It is likely that these large rectangular complexes would be taken up more efficiently by tumor cells,[32] which are permeable to large, non-natural molecules, whereas healthy cells are less able to take up such structures, which should provide a degree of selectivity and ultimately lead to reduced drug side effects.

(32) Modi, S.; Jain, J. P.; Domb, A. J.; Kumar, N. *Curr. Pharm. Des.* **2006**, *12*, 4785–4796.

Experimental Section

General Remarks. The dinuclear arene ruthenium complexes [Ru_2(arene)$_2$($OO\cap OO$)Cl_2] (arene = *p*-cymene, hexamethylbenzene; $OO\cap OO$ = 2,5-dihydroxy-1,4-benzoquinonato, 2,5-dichloro-1,4-benzoquinonato) (**1**−**4**) were prepared according to published methods.[24,25] All other reagents were commercially available and used as received. The ^1H and $^{13}C\{^1H\}$ NMR spectra were recorded on a Bruker AMX 400 spectrometer using the residual protonated solvent as internal standard (acetone-d_6: δ_H = 2.09 ppm). Infrared spectra were recorded as KBr pellets on a Perkin-Elmer FTIR 1720-X spectrometer. Microanalyses were performed by the Laboratory of Pharmaceutical Chemistry, University of Geneva (Switzerland).

General Synthetic Method for [9−16][CF_3SO_3]$_4$. A mixture of **1**−**4** (0.1 mmol) and 2 equiv of $AgCF_3SO_3$ (0.2 mmol) in methanol (20 mL) is stirred at room temperature for 2 h and then filtered to remove AgCl. To the red filtrate, the corresponding $N\cap N$ ligand (0.1 mmol) is added. The mixture is stirred at room temperature for 24 h, and the solvent is removed under vacuum. The residue is taken up in dichloromethane (20 mL), the extract is filtered and concentrated (3 mL), and diethyl ether

is slowly added to precipitate the product as a dark orange or red solid.

[Ru_4(*p*-cymene)$_4$(pyrazine)$_2$(2,5-dihydroxy-1,4-benzoquinonato)$_2$][CF_3SO_3]$_4$ ([5][CF_3SO_3]$_4$). Yield: 0.036 mmol (72%). ^{1}H NMR (400 MHz, acetone-d_6): δ (ppm) 8.70 (s, 8H, CH_{pyz}), 6.21 (d, 8H, $^3J_{H-H}$ = 6.4 Hz, C$H_{p\text{-cym}}$), 6.05 (d, 8H, $^3J_{H-H}$ = 6.4 Hz, C$H_{p\text{-cym}}$), 5.64 (s, 4H, CH_{dbq}), 2.96 (sep, 4H, $^3J_{H-H}$ = 7.0 Hz, CH(CH_3)$_2$), 2.35 (s, 12H, CH_3), 1.39 (d, 24H, $^3J_{H-H}$ = 7.0 Hz, CH(CH_3)$_2$). ^{13}C{^{1}H} NMR (100 MHz, acetone-d_6): δ (ppm) 184.8 (*C*=O), 149.9 (*C*H$_{pyz}$), 104.8 (*C*$_{p\text{-cym}}$), 102.1 (*C*H$_{dbq}$), 98.5 (*C*$_{p\text{-cym}}$), 83.8 (*C*H$_{p\text{-cym}}$), 83.2 (*C*H$_{p\text{-cym}}$), 31.1 (*C*H(CH$_3$)$_2$), 21.1 (*C*H$_3$), 16.5 (CH(*C*H$_3$)$_2$). IR (cm^{-1}): 1637(w), 1529(s), 1377(m), 1259(s), 1227(w), 1162(m), 1030(m), 635(w). Anal. Calcd for $C_{64}H_{68}N_4O_{20}F_{12}S_4Ru_4$: C, 38.95; H, 3.47; N, 2.84. Found: C, 38.73; H, 3.44; N, 2.78.

[Ru_4(*p*-cymene)$_4$(pyrazine)$_2$(2,5-dichloro-1,4-benzoquinonato)$_2$][CF_3SO_3]$_4$ ([6][CF_3SO_3]$_4$). Yield: 0.034 mmol (68%). ^{1}H NMR (400 MHz, acetone-d_6): δ (ppm) 8.75 (s, 8H, CH_{pyz}), 6.30 (d, 8H, $^3J_{H-H}$ = 6.4 Hz, C$H_{p\text{-cym}}$), 6.14 (d, 8H, $^3J_{H-H}$ = 6.4 Hz, C$H_{p\text{-cym}}$), 3.06 (sep, 4H, $^3J_{H-H}$ = 6.9 Hz, CH(CH$_3$)$_2$), 2.44 (s, 12H, CH_3), 1.46 (d, 24H, $^3J_{H-H}$ = 6.9 Hz, CH(CH_3)$_2$). ^{13}C{^{1}H} NMR (100 MHz, acetone-d_6): δ (ppm) 177.9 (*C*=O), 150.3 (*C*H$_{pyz}$), 106.1 (*C*$_{p\text{-cym}}$), 104.5 (*C*$_{dbq}$), 98.8 (*C*$_{p\text{-cym}}$), 84.1 (*C*H$_{p\text{-cym}}$), 83.9 (*C*H$_{p\text{-cym}}$), 31.3 (*C*H(CH$_3$)$_2$), 21.4 (*C*H$_3$), 17.3 (CH(*C*H$_3$)$_2$). IR (cm^{-1}): 1627(w), 1504(s), 1373(s), 1266(s), 1225(w), 1163(m), 1029(m), 637(m). Anal. Calcd for $C_{64}H_{64}Cl_4N_4O_{20}F_{12}S_4Ru_4\cdot CH_2Cl_2$: C, 35.54; H, 3.03; N, 2.55. Found: C, 35.08; H, 3.17; N, 2.69.

[Ru_4(hexamethylbenzene)$_4$(pyrazine)$_2$(2,5-dihydroxy-1,4-benzoquinonato)$_2$][CF_3SO_3]$_4$ ([7][CF_3SO_3]$_4$). Yield: 0.042 mmol (83%). ^{1}H NMR (400 MHz, acetone-d_6): δ (ppm) 8.70 (s, 8H, CH_{pyz}), 5.72 (s, 4H, CH_{dbq}), 2.20 (s, 72H, CH_3). ^{13}C{^{1}H} NMR (100 MHz, acetone-d_6): δ (ppm) 183.9 (*C*=O), 148.0 (*C*H$_{pyz}$), 101.7 (*C*H$_{dbq}$), 93.7 (*C*$_{hmb}$), 14.6 (*C*H$_3$). IR (cm^{-1}): 1628(w), 1527(s), 1374(s), 1257(s), 1224(w), 1156(m), 1031(m), 638(m). Anal. Calcd for $C_{72}H_{84}N_4O_{20}F_{12}S_4Ru_4\cdot CH_2Cl_2$: C, 40.39; H, 3.99; N, 2.58. Found: C, 39.85; H, 4.01; N, 2.70.

[Ru_4(hexamethylbenzene)$_4$(pyrazine)$_2$(2,5-dichloro-1,4-benzoquinonato)$_2$][CF_3SO_3]$_4$ ([8][CF_3SO_3]$_4$). Yield: 0.037 mmol (75%). ^{1}H NMR (400 MHz, acetone-d_6): δ (ppm) 8.71 (s, 8H, CH_{pyz}), 2.21 (s, 72H, CH_3). ^{13}C{^{1}H} NMR (100 MHz, acetone-d_6): δ (ppm) 183.8 (*C*=O), 148.0 (*C*H$_{pyz}$), 105.3 (*C*$_{dbq}$), 93.7 (*C*$_{hmb}$), 14.6 (*C*H$_3$). IR (cm^{-1}): 1626(w), 1504(s), 1372(m), 1260 (m) 1158(w), 1031(m), 638(w). Anal. Calcd for $C_{72}H_{80}Cl_4N_4O_{20}F_{12}S_4Ru_4$: C, 38.89; H, 3.63; N, 2.52. Found: C, 38.63; H, 3.77; N, 2.45.

[Ru_4(*p*-cymene)$_4$(4,4′-bipyridine)$_2$(2,5-dihydroxy-1,4-benzoquinonato)$_2$][CF_3SO_3]$_4$ ([9][CF_3SO_3]$_4$). Yield: 0.037 mmol (74%). ^{1}H NMR (400 MHz, acetone-d_6): δ (ppm) 8.54 (d, 8H, $^3J_{H-H}$ = 4.4 Hz, CH_{bpy}), 8.02 (d, 8H, $^3J_{H-H}$ = 4.4 Hz, CH_{bpy}), 6.20 (d, 8H, $^3J_{H-H}$ = 8.0 Hz, C$H_{p\text{-cym}}$), 5.99 (d, 8H, $^3J_{H-H}$ = 8.0 Hz, C$H_{p\text{-cym}}$), 5.79 (s, 4H, CH_{dbq}), 2.95 (sep, 4H, $^3J_{H-H}$ = 8.0 Hz, CH(CH$_3$)$_2$), 2.21 (s, 12H, CH_3), 1.38 (d, 24H, $^3J_{H-H}$ = 8.0 Hz, CH(CH_3)$_2$). ^{13}C{^{1}H} NMR (100 MHz, acetone-d_6): δ (ppm) 174.3 (*C*=O), 154.0 (*C*H$_{bpy}$), 144.7 (*C*$_{bpy}$), 123.6 (*C*H$_{bpy}$), 103.7 (*C*$_{p\text{-cym}}$), 101.7 (*C*H$_{dbq}$), 99.3 (*C*$_{p\text{-cym}}$), 83.9 (*C*H$_{p\text{-cym}}$), 82.1 (*C*H$_{p\text{-cym}}$), 31.2 (*C*H(CH$_3$)$_2$), 21.6 (*C*H$_3$), 17.2 (CH(*C*H$_3$)$_2$). IR (cm^{-1}): 1637(s), 1616(s), 1526(m), 1378(s), 1259(m), 1159(s), 1030(s), 636(s). Anal. Calcd for $C_{76}H_{76}N_4O_{20}F_{12}S_4Ru_4$: C, 42.94; H, 3.60; N, 2.64. Found: C, 42.91; H, 3.87; N, 2.61.

[Ru_4(*p*-cymene)$_4$(4,4′-bipyridine)$_2$(2,5-dichloro-1,4-benzoquinonato)$_2$][CF_3SO_3]$_4$ ([10][CF_3SO_3]$_4$). Yield: 0.038 mmol (75%). ^{1}H NMR (400 MHz, acetone-d_6): δ (ppm) 8.54 (d, 8H, $^3J_{H-H}$ = 6.4 Hz, CH_{bpy}), 8.06 (d, 8H, $^3J_{H-H}$ = 6.4 Hz, CH_{bpy}), 6.28 (d, 8H, $^3J_{H-H}$ = 6.4 Hz, C$H_{p\text{-cym}}$), 6.11 (d, 8H, $^3J_{H-H}$ = 6.4 Hz, C$H_{p\text{-cym}}$), 2.99 (sep, 4H, $^3J_{H-H}$ = 6.8 Hz, CH(CH$_3$)$_2$), 2.34 (s, 12H, CH_3), 1.42 (d, 24H, $^3J_{H-H}$ = 6.8 Hz, CH(CH_3)$_2$). ^{13}C{^{1}H} NMR (100 MHz, acetone-d_6): δ (ppm) 178.5 (*C*=O), 154.8 (*C*H$_{bpy}$), 145.6 (*C*$_{bpy}$), 124.6 (*C*H$_{bpy}$), 107.0 (*C*$_{p\text{-cym}}$), 104.8 (*C*$_{dbq}$), 100.1 (*C*$_{p\text{-cym}}$), 84.9 (*C*H$_{p\text{-cym}}$), 83.8 (*C*H$_{p\text{-cym}}$), 32.2 (*C*H(CH$_3$)$_2$), 22.5 (*C*H$_3$), 18.2 (CH(*C*H$_3$)$_2$). IR (cm^{-1}): 1637(s), 1617(s) 1502(m) 1374(m), 1259(s), 1163(m), 1031(s) 638(s). Anal. Calcd for $C_{76}H_{72}N_4O_{20}F_{12}S_4Cl_4Ru_4$: C, 40.32; H, 3.21; N, 2.47. Found: C, 40.85; H, 3.32; N, 2.36.

[Ru_4(hexamethylbenzene)$_4$(4,4′-bipyridine)$_2$(2,5-dihydroxy-1,4-benzoquinonato)$_2$][CF_3SO_3]$_4$ ([11][CF_3SO_3]$_4$). Yield: 0.027 mmol (54%). ^{1}H NMR (400 MHz, acetone-d_6): δ (ppm) 8.39 (d, 8H, $^3J_{H-H}$ = 5.3 Hz, CH_{bpy}), 8.08 (d, 8H, $^3J_{H-H}$ = 5.3 Hz, CH_{bpy}), 5.76 (s, 4H, CH_{dbq}), 2.16 (s, 72H, CH_3). ^{13}C{^{1}H} NMR (100 MHz, acetone-d_6): δ (ppm) 175.2 (*C*=O), 153.4 (*C*H$_{bpy}$), 144.1 (*C*$_{bpy}$), 123.6 (*C*H$_{bpy}$), 101.7 (*C*H$_{dbq}$), 93.6 (*C*$_{hmb}$), 14.7 (*C*H$_3$). IR (cm^{-1}): 1638(s), 1617(s), 1525(s), 1375(m), 1258(s), 1162(m), 1032(s), 622(s). Anal. Calcd for $C_{84}H_{92}N_4O_{20}F_{12}S_4Ru_4$: C, 45.08; H, 4.14; N, 2.50. Found: C, 45.01; H, 4.14; N, 2.32.

Crystals suitable for X-ray diffraction analysis were obtained by slow diffusion of diethyl ether in an acetone solution of [**11**][CF_3SO_3]$_4$.

[Ru_4(hexamethylbenzene)$_4$(4,4′-bipyridine)$_2$(2,5-dichloro-1,4-benzoquinonato)$_2$][CF_3SO_3]$_4$ ([12][CF_3SO_3]$_4$). Yield: 0.036 mmol (73%). ^{1}H NMR (400 MHz, acetone-d_6): δ (ppm) 8.40 (dd, 8H, $^3J_{H-H}$ = 5.4 Hz, $^4J_{H-H}$ = 1.5 Hz, CH_{bpy}), 8.13 (dd, 8H, $^3J_{H-H}$ = 5.4 Hz, $^4J_{H-H}$ = 1.5 Hz, CH_{bpy}), 2.18 (s, 72H, CH_3). ^{13}C{^{1}H} NMR (100 MHz, acetone-d_6): δ (ppm) 177.5 (*C*=O), 153.8 (*C*H$_{bpy}$), 144.6 (*C*$_{bpy}$), 126.7 (*C*H$_{bpy}$), 106.4 (*C*$_{dbq}$), 94.4 (*C*$_{hmb}$), 15.2 (*C*H$_3$). IR (cm^{-1}): 1637(s), 1617(s), 1499(s), 1369(m), 1259(s), 1161(m), 1032(s), 638(s). Anal. Calcd for $C_{84}H_{88}N_4O_{20}F_{12}S_4Cl_4Ru_4$: C, 42.46; H, 3.73; N, 2.36. Found: C, 42.44; H, 3.23; N, 2.32.

[Ru_4(*p*-cymene)$_4${1,2-bis(4-pyridyl)ethylene}$_2$(2,5-dihydroxy-1,4-benzoquinonato)$_2$][CF_3SO_3]$_4$ ([13][CF_3SO_3]$_4$). Yield: 0.040 mmol (80%). ^{1}H NMR (400 MHz, acetone-d_6): δ (ppm) 8.35 (d, 8H, $^3J_{H-H}$ = 6.6 Hz, CH_{bpe}), 7.74 (d, 8H, $^3J_{H-H}$ = 6.6 Hz, CH_{bpe}), 7.63 (s, 4H, CH_{bpe}), 6.17 (d, 8H, $^3J_{H-H}$ = 6.4 Hz, C$H_{p\text{-cym}}$), 5.98 (d, 8H, $^3J_{H-H}$ = 6.4 Hz, C$H_{p\text{-cym}}$), 5.78 (s, 4H, CH_{dbq}), 2.96 (sep, 4H, $^3J_{H-H}$ = 7.1 Hz, CH(CH$_3$)$_2$), 2.23 (s, 12H, CH_3), 1.36 (d, 24H, $^3J_{H-H}$ = 7.1 Hz, CH(CH_3)$_2$). ^{13}C{^{1}H} NMR (100 MHz, acetone-d_6): δ (ppm) 184.2 (*C*=O), 153.2 (*C*H$_{bpe}$), 146.1 (*C*$_{bpe}$), 131.7 (*C*H$_{bpe}$), 123.9 (*C*H$_{bpe}$), 103.7 (*C*$_{p\text{-cym}}$), 101.7 (*C*H$_{dbq}$), 99.0 (*C*$_{p\text{-cym}}$), 83.7 (*C*H$_{p\text{-cym}}$), 82.1 (*C*H$_{p\text{-cym}}$), 31.2 (*C*H(CH$_3$)$_2$), 21.6 (*C*H$_3$), 17.2 (CH(*C*H$_3$)$_2$). IR (cm^{-1}): 1638(s), 1616 (s), 1525(s), 1378(m), 1259(m), 1161(m), 1031(m), 636(s). Anal. Calcd for $C_{80}H_{80}N_4O_{20}F_{12}S_4Ru_4$: C, 44.12; H, 3.70; N, 2.57. Found: C, 44.06; H, 3.86; N, 2.55.

[Ru_4(*p*-cymene)$_4${1,2-bis(4-pyridyl)ethylene}$_2$(2,5-dichloro-1,4-benzoquinonato)$_2$][CF_3SO_3]$_4$ ([14][CF_3SO_3]$_4$). Yield: 0.037 mmol (74%). ^{1}H NMR (400 MHz, acetone-d_6): δ (ppm) 8.32 (dd, 8H, $^3J_{H-H}$ = 5.4 Hz, $^4J_{H-H}$ = 1.4 Hz, CH_{bpe}), 7.77 (dd, 8H, $^3J_{H-H}$ = 5.4 Hz, $^4J_{H-H}$ = 1.4 Hz, CH_{bpe}), 7.69 (s, 4H, CH_{bpe}), 6.25 (d, 8H, $^3J_{H-H}$ = 6.4 Hz, C$H_{p\text{-cym}}$), 6.08 (d, 8H, $^3J_{H-H}$ = 6.4 Hz, C$H_{p\text{-cym}}$), 3.03 (sep, 4H, $^3J_{H-H}$ = 7.0 Hz, CH(CH$_3$)$_2$), 2.32 (s, 12H, CH_3), 1.42 (d, 24H, $^3J_{H-H}$ = 7.0 Hz, CH(CH_3)$_2$). ^{13}C{^{1}H} NMR (100 MHz, acetone-d_6): δ (ppm) 178.0 (*C*=O), 153.3 (*C*H$_{bpe}$), 146.4 (*C*$_{bpe}$), 132.0 (*C*H$_{bpe}$), 124.2 (*C*H$_{bpe}$), 106.2 (*C*$_{p\text{-cym}}$), 104.0 (*C*$_{dbq}$), 99.0 (*C*$_{p\text{-cym}}$), 83.9 (*C*H$_{p\text{-cym}}$), 82.9 (*C*H$_{p\text{-cym}}$), 31.4 (*C*H(CH$_3$)$_2$), 21.7 (*C*H$_3$), 17.4 (CH(*C*H$_3$)$_2$). IR (cm^{-1}): 1638(s), 1619(s), 1501(s), 1373(m), 1258(s), 1163(m), 1031(m), 638(s). Anal. Calcd for $C_{80}H_{76}N_4O_{20}F_{12}S_4Cl_4Ru_4$: C, 41.49; H, 3.31; N, 2.42. Found: C, 41.43; H, 3.49; N, 2.26.

[Ru_4(hexamethylbenzene)$_4${1,2-bis(4-pyridyl)ethylene}$_2$(2,5-dihydroxy-1,4-benzoquinonato)$_2$][CF_3SO_3]$_4$ ([15][CF_3SO_3]$_4$). Yield: 0.041 mmol (83%). ^{1}H NMR (400 MHz, acetone-d_6): δ (ppm) 8.20 (dd, 8H, $^3J_{H-H}$ = 5.4 Hz, $^4J_{H-H}$ = 1.4 Hz, CH_{bpe}), 7.76 (dd, 8H, $^3J_{H-H}$ = 5.4 Hz, $^4J_{H-H}$ = 1.4 Hz, CH_{bpe}), 7.59 (s, 4H, CH_{bpe}), 5.76 (s, 4H, CH_{dbq}), 2.15 (s, 72H, CH_3). ^{13}C{^{1}H} NMR (100 MHz, acetone-d_6): δ (ppm) 184.6 (*C*=O), 153.5 (*C*H$_{bpe}$), 146.9 (*C*$_{bpe}$), 132.6 (*C*H$_{bpe}$), 125.2 (*C*H$_{bpe}$), 102.7 (*C*H$_{dbq}$), 94.3 (*C*$_{hmb}$), 15.6 (*C*H$_3$). IR (cm^{-1}): 1638(s), 1617(s), 1524(m), 1374(m), 1257(m), 1112(m), 1031(m), 621(s). Anal. Calcd for $C_{88}H_{96}N_4O_{20}F_{12}S_4Ru_4$: C, 46.15; H, 4.22; N, 2.45. Found: C, 46.32; H, 4.46; N, 2.29.

Table 3. Crystallographic and Structure Refinement Parameters for Compounds [11][CF_3SO_3]$_4$ and [16][CF_3SO_3]$_4$·($C_4H_{10}O$)$_2$·(C_3H_6O)$_2$

	[**11**][CF_3SO_3]$_4$	[**16**][CF_3SO_3]$_4$·solvent
chemical formula	$C_{102}H_{124}Cl_4F_{12}N_4O_{24}Ru_4S_4$	$C_{84}H_{92}F_{12}N_4O_{20}Ru_4S_4$
fw	2692.37	2238.14
cryst syst	triclinic	monoclinic
space group	$P\bar{1}$ (no. 2)	$P2/m$ (no. 10)
cryst color and shape	orange block	red block
cryst size	0.13 × 0.10 × 0.08	0.14 × 0.12 × 0.10
a (Å)	13.9532(7)	15.2127(11)
b (Å)	15.4561(8)	9.9525(5)
c (Å)	15.8403(9)	20.6506(14)
α (deg)	66.311(4)	90
β (deg)	64.864(4)	109.011(5)
γ (deg)	76.075(4)	90
V (Å^3)	2822.0(3)	2956.1(3)
Z	1	1
T (K)	173(2)	173(2)
D_c (g·cm^{-3})	1.584	1.257
μ (mm^{-1})	0.784	0.645
scan range (deg)	2.88 < 2θ < 51.28	2.84 < 2θ < 50.32
unique reflns	10 619	5565
reflns used [$I > 2\sigma(I)$]	9210	4146
R_{int}	0.0438	0.0773
final R indices [$I > 2\sigma(I)$][a]	R_1 0.0319, wR_2 0.0815	R_1 0.0450, wR_2 0.1251
R indices (all data)	R_1 0.0381, wR_2 0.0839	R_1 0.0596, wR_2 0.1309
goodness-of-fit	1.019	0.981
max., min. $\Delta\rho$ (e Å^{-3})	0.619, −0.608	0.478, −0.686

[a] Structures were refined on F_o^2: $wR_2 = [\sum[w(F_o^2 - F_c^2)^2]/\sum w(F_o^2)^2]^{1/2}$, where $w^{-1} = [\sum(F_o^2) + (aP)^2 + bP]$ and $P = [\max(F_o^2, 0) + 2F_c^2]/3$.

[Ru$_4$(hexamethylbenzene)$_4${1,2-bis(4-pyridyl)ethylene}$_2$(2,5-dichloro-1,4-benzoquinonato)$_2$][CF_3SO_3]$_4$ ([16][CF_3SO_3]$_4$). Yield: 0.033 mmol (66%). ^{1}H NMR (400 MHz, acetone-d_6): δ (ppm) 8.19 (dd, 8H, $^3J_{H-H}$ = 6.6 Hz, $^4J_{H-H}$ = 1.2 Hz, CH_{bpe}), 7.80 (dd, 8H, $^3J_{H-H}$ = 6.6 Hz, $^4J_{H-H}$ = 1.2 Hz, CH_{bpe}), 7.67 (s, 4H, CH_{bpe}), 2.18 (s, 72H, CH_3). ^{13}C{^{1}H} NMR (100 MHz, acetone-d_6): δ (ppm) 177.5 (*C*=O), 152.6 (*C*H$_{bpe}$), 146.2 (*C*$_{bpe}$), 131.9 (*C*H$_{bpe}$), 124.4 (*C*H$_{bpe}$), 106.0 (*C*$_{dbq}$), 93.7 (*C*$_{hmb}$), 14.7 (*C*H$_3$). IR (cm^{-1}): 1638(s), 1617(s), 1498(s), 1370(m), 1164(m), 1031(m), 623(s). Anal. Calcd for $C_{88}H_{92}N_4O_{20}F_{12}S_4Cl_4Ru_4$: C, 43.53; H, 3.82; N, 2.31. Found: C, 43.92; H, 3.94; N, 2.25.

Crystals suitable for X-ray diffraction analysis were obtained by slow diffusion of diethyl ether in an acetone solution of [**16**][CF_3SO_3]$_4$.

Electrochemistry. Electrochemical measurements were carried out with a computer-controlled multipurpose potentiostat μAUTOLAB III (Eco Chemie) at room temperature using a standard Metrohm three-electrode cell with platinum disk electrode (AUTOLAB RDE; 3 mm diameter) as the working electrode, platinum sheet auxiliary electrode, and calomel reference electrode (3 M KCl). The analyzed compounds were dissolved in dichloromethane (Fluka, absolute, declared H_2O content ≤0.005%) to give a solution containing 5×10^{-4} M of the analyte and 0.1 M Bu_4NPF_6 (Fluka, purissimum for electrochemistry). In the case of poorly soluble compounds, saturated solutions were used. The solutions were deaerated with argon prior to the measurement and then kept under an argon blanket. The redox potentials are given relative to the ferrocene/ferrocenium reference and are reproducible within ca. ±5 mV.

Cytotoxicity Study. The human A2780 ovarian cancer cell line was obtained from the European Collection of Cell Cultures (Salisbury, UK). Cells were grown routinely in RPMI medium containing glucose, 5% fetal calf serum (FCS), and antibiotics at 37 °C and 5% CO_2. Cytotoxicity was determined using the MTT assay (MTT = 3-(4,5-dimethyl-2-thiazolyl)-2,5-diphenyl-2*H*-tetrazolium bromide).[33] Cells were seeded in 96-well plates as monolayers with 100 μL of cell solution (approximately 20 000 cells) per well and preincubated for 24 h in medium supplemented with 10% FCS. Compounds were predissolved in DMSO, then added to the culture medium (to give a final DMSO concentration of 0.5%) and serially diluted to the appropriate concentration; 100 μL of drug solution was added to each well, and the plates were incubated for another 72 h. Subsequently, MTT (5 mg/mL solution) was added to the cells, and the plates were incubated for a further 2 h. The culture medium was aspirated, and the purple formazan crystals formed by the mitochondrial dehydrogenase activity of vital cells were dissolved in DMSO. The optical density, directly proportional to the number of surviving cells, was quantified at 540 nm using a multiwell plate reader, and the fraction of surviving cells was calculated from the absorbance of untreated control cells. Evaluation is based on means from two independent experiments, each comprising 3 microcultures per concentration level.

X-ray Crystallographic Study. Crystals of [**11**][CF_3SO_3]$_4$ and [**16**][CF_3SO_3]$_4$·($C_4H_{10}O$)$_2$·(C_3H_6O)$_2$ were mounted on a Stoe Image Plate Diffraction system equipped with a ϕ circle goniometer, using Mo Kα graphite-monochromated radiation (λ = 0.71073 Å) with ϕ range 0−200°, increment of 1.2° and 1.0°, respectively, 2θ range from 4.0° to 52°, $D_{max} - D_{min}$ = 12.45−0.81 Å. The structures were solved by direct methods using the program SHELXS-97.[34] Refinement and all further calculations were carried out using SHELXL-97.[34] Examination of the structures with PLATON[35] reveals in [**11**][CF_3SO_3]$_4$ voids between the anions and cations. Therefore, a new data set corresponding to omission of the missing solvent and anions was generated with the SQUEEZE algorithm,[36] and the structure was refined to convergence. Otherwise, in both structures, the H atoms were included in calculated positions and treated as riding atoms using the SHELXL default parameters, and the non H atoms were refined anisotropically, using weighted full-matrix least-squares on F^2. Crystallographic details are summarized in Table 3. Figures 1 and 2 are drawn with ORTEP,[37] while Figure 3 is drawn with MERCURY.[38]

CCDC-721012 [**11**][CF_3SO_3]$_4$ and 721013 [**16**][CF_3SO_3]$_4$·($C_4H_{10}O$)$_2$·(C_3H_6O)$_2$ contain the supplementary crystallographic data for this paper. These data can be obtained free of charge at www.ccdc.cam.ac.uk/conts/retrieving.html [or from the Cambridge Crystallographic Data Centre, 12 Union Road, Cambridge CB2 1EZ, UK; fax: (internat.) +44-1223/336-033; E-mail: deposit@ccdc.cam.ac.uk].

Acknowledgment. We thank Johnson Matthey Research Centre for a generous loan of ruthenium chloride hydrate and the Swiss National Science Foundation for financial support. This work is part of the long-term research project of the Faculty of Science, Charles University, supported by the Ministry of Education of the Czech Republic (project no. MSM0021620857).

Supporting Information Available: X-ray data given as CIF files. This material is available free of charge via the Internet at http://pubs.acs.org

(33) Mosmann, T. *J. Immunol. Methods* **1983**, *65*, 55–63.
(34) Sheldrick, G. M. *Acta Crystallogr.* **2008**, *A64*, 112–122.
(35) Spek, A. L. *J. Appl. Crystallogr.* **2003**, *36*, 7–13.
(36) van der Sluis, P.; Spek, A. L. *Acta Crystallogr.* **1990**, *A46*, 194–201.
(37) Farrugia, L. J. *J. Appl. Crystallogr.* **1997**, *30*, 565.
(38) Macrae, C. F.; Edgington, P. R.; McCabe, P.; Pidcock, E.; Shields, G. P.; Taylor, R.; Towler, M.; van de Streek, J. *J. Appl. Crystallogr.* **2006**, *39*, 453–457.